

Adaptive Tracking of Electronic Communication Signals Based on Nonlinear Filtering

Zailin Li*

School of 3d Printing, Xinxiang University, Xinxiang, 453000, China

With the rapid development of the Internet, people have increased their network interaction behaviors in indoor environments, and indoor positioning services are being used more and more frequently in daily life. The TC-OFDM system has shown good performance in indoor positioning applications in recent years, and the gradual progress of 5G technology and the wide application of Time Division Duplex (TDD) technology require a new method for the existing TC-OFDM indoor positioning system. The intermittent broadcast of 5G signals in TDD makes it difficult for the existing TC-OFDM system receiver to effectively track the positioning signal. In this regard, the open-loop structure is used to redesign the signal tracking loop of the TC-OFDM receiver. In this paper, an improved adaptive Kalman filtering algorithm (Kalman filtering, KF) is introduced. The simulation results show that the open-loop tracking structure has a faster convergence speed when tracking the TC-OFDM signal, and the accuracy is demonstrably higher than that of the traditional closed-loop. Hence, the adaptive KF makes the receiver well suited for applications with low CNR and environments with large signal fluctuations.

Keywords: Adaptive Kalman filter; communication system; open loop; signal tracking

1. INTRODUCTION

Electronic communication technology has gradually matured after decades of development, and has continuously advanced the informatization process in society. Among them, wireless communication technology has been widely used in many fields [1]. As the representative of the wireless communication system, the mobile communication system has developed rapidly in recent years, and has provided many modern services that have a profound impact on people's lifestyles, among which navigation and positioning services are the representatives. The improvement of satellite navigation technology has made the outdoor high-precision positioning level higher and higher, while indoor positioning is not ideal due to the complex environment and many obstacles [2]. The rapid development of mobile communication technology has promoted the realization of precise positioning

in indoor environments, and achieved good results. At the same time, based on Orthogonal Frequency Division Multiplexing (OFDM) and 5th Generation Mobile Communication Technology, 5G) and other emerging technologies, modern mobile communication systems make it possible to achieve new breakthroughs in indoor positioning. The TC-OFDM (TimeCode Division-Orthogonal Frequency Division Multiplexing) positioning system independently developed in China performs well in indoor positioning, although to ensure a good positioning outcome of the system, the signal processing technology of the receiver is very critical [3]. Also, with the gradual popularization of 5G, the performance of the receiver is in urgent need of greater improvement. The carrier tracking loop design of the receiver has a significant impact on its performance. In this paper, an adaptive Kalman filter tracking algorithm is designed to improve the intermittent signal tracking loop of the receiver, thereby improving the performance and TC-Positioning effect of OFDM of the receiver.

*Email of corresponding author: zailinli@163.com

2. RELATED WORKS

Wireless communication systems can be divided into digital communication systems and analog communication systems. In the two systems, the sender and the receiver are usually in two different places. In order to ensure the correct exchange of information at both ends, an accurate and efficient synchronization system must be established. Synchronization issues are critical. Carrier synchronization is divided into two synchronization stages: carrier acquisition and tracking. Of these, the carrier tracking is directly related to the design of the receiver's tracking loop. Only when the receiver's tracking loop is properly designed can high-precision carrier synchronization be achieved [4]. The traditional carrier tracking loop is usually divided into phase locked loop (PLL) and frequency locked loop (FLL) systems, which many researchers have sought to improve and innovate. For the phase-locked loop structure of the minimum frequency shift keying receiver, Dong et al. [5] used a CMOS process mixer, and used double-balanced anti-parallel diodes for phase detection to reduce the oscillator frequency. As a result, the receiver achieves self-synchronization of the carrier frequency, and achieves a bit error rate of 10 Gb/s and a maximum data rate of 12.5 Gb/s. Focusing on the carrier tracking error or loss of lock of TC-OFDM receiver caused by carrier-to-noise ratio, Mo et al. [6] proposed a fuzzy control frequency-locked loop for auxiliary phase-locked loop, and designed a second-order frequency-locked loop by using Kalman filter. Auxiliary third-order phase-locked loop tracking loop. The simulation results show that this method can effectively avoid loss of lock compared with the traditional method, and the accuracy and robustness are significantly improved. Yang et al. [7] designed a frequency-locked loop based on the decentralized state estimation framework to assist the phase-locked loop to improve the tracking performance of the GNSS carrier loop. The carrier tracking loop under this framework has good phase performance. Compared with the carrier tracking loop of the centralized framework, the carrier tracking loop of the decentralized framework is more robust in weak signal and high dynamic scenarios. Xu et al. [8] adopted global synchronous pulse width modulation and proposed a carrier synchronization method with a phase-locked loop structure. Using this method, the coordinated control of switching sequences can be achieved without relying on a low-latency communication system, thereby effectively improving the global communication rate. The adaptability of synchronous PWM carrier synchronization, and the hardware cost is significantly reduced. Liu et al. [9] proposed a new MQAM (Multiple Quadrature Amplitude Modulation, MQAM) method using the improved Gardner algorithm, which estimates the timing offset and carrier offset by means of the Gardner algorithm, and then uses the phase-locked loop mechanism monitors the frequency offset and phase offset, thereby solving the symbol timing and carrier synchronization problems of MQAM signals when there are large symbol rate deviations in multipath channels.

Many scholars have proposed tracking algorithms to replace traditional tracking loops by using signal parameter estimation. Among them, the tracking algorithm based

on Kalman filter has good tracking performance and can be applied to carrier tracking in complex environments containing high dynamics and weak signals. research hotspots in the field. Cheng and Chang [10] pointed out that the traditional Kalman filter has poor performance in tracking weak signals due to the defect of prior noise covariance. Therefore, an adaptive Kalman filter carrier tracking method is proposed. The noise covariance is updated synchronously in real time. The method was successfully applied to the receiver, and compared with the traditional Kalman filter, showing better weak-signal tracking sensitivity and significantly reducing the convergence time. Cheng and Chang [11] also introduced an attenuation factor into the state prediction covariance of the Kalman filter to adjust the Kalman gain, and adjusted the measurement noise covariance based on the carrier-to-noise ratio estimate to improve the accuracy of the attenuation factor. Compared with traditional methods, with this method, the receiver shows stronger adaptability in complex environments, and the tracking performance is significantly improved. Chen et al. [12] used online variance component estimation to dynamically update the noise in the Kalman filter process, and combined the least squares ionospheric delay modeling method to achieve code pseudo-range and carrier phase measurements. Simulation experiments demonstrated that the method can effectively simulate the ionospheric delay variation under different sampling intervals, and the positioning accuracy in the three directions of North (North), East (East), and High (Up) is improved by 21%, 35% and 16% compared with the original data set respectively. Tang et al. [13] proposed a clear tuning rule for the parameters of the Kalman filter, thereby improving the mathematical expression of the Kalman gain and proposing a corresponding tracking model to achieve the tuning of the Kalman filter. Experiments on different receivers show that the adjustment rule is reasonable, the adjusted signal parameters are accurate and reliable, and the difficulty of subsequent processing is effectively reduced. Cheng et al. [14] proposed a tracking loop based on a two-stage Kalman filter, which avoids the limitation of the bit sign when increasing the coherent integration time, thereby effectively improving the tracking sensitivity and the tracking performance for weak signals. Jin et al. [15] proposed an open-loop tracking structure based on differential Kalman filter for GNSS in urban complex environment. In road experiments, the open-loop tracking structure improves the tracking accuracy by more than 50% compared with the traditional structure.

The traditional carrier tracking loop has a good tracking effect on stable signals, but has poor adaptability in dynamic environments and is greatly affected by the pulling range, so it is not effective in tracking intermittently broadcast signals. The Kalman filter estimation result based on signal parameter estimation depends on real-time measurement data and is not easily affected by the DutyRatio, but the measurement and the estimation accuracy need to be improved. The adaptive improvement of the Kalman filter, combined with the open-loop tracking structure, can effectively improve the tracking effect of intermittently-broadcast positioning signals.

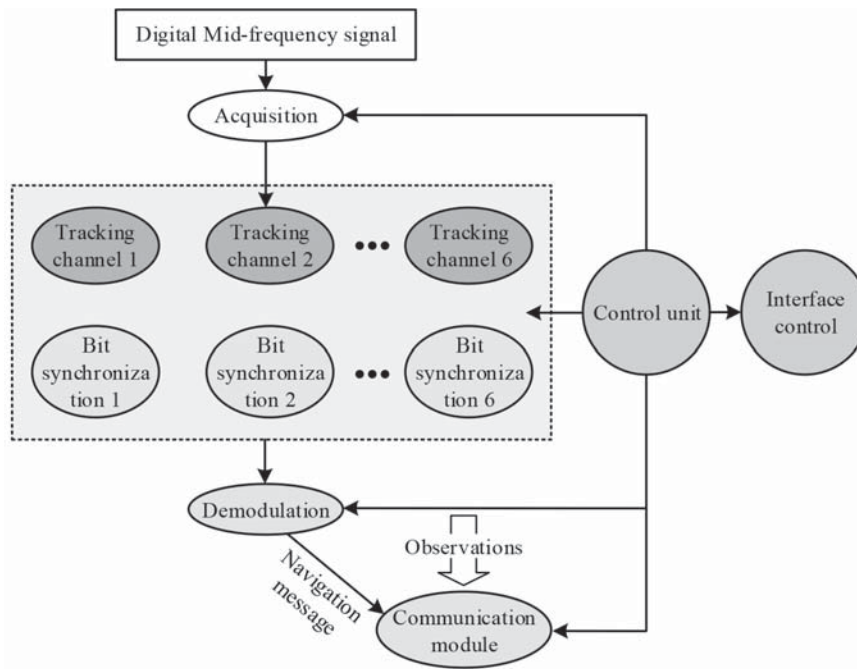


Figure 1 Signal processing process of receiver.

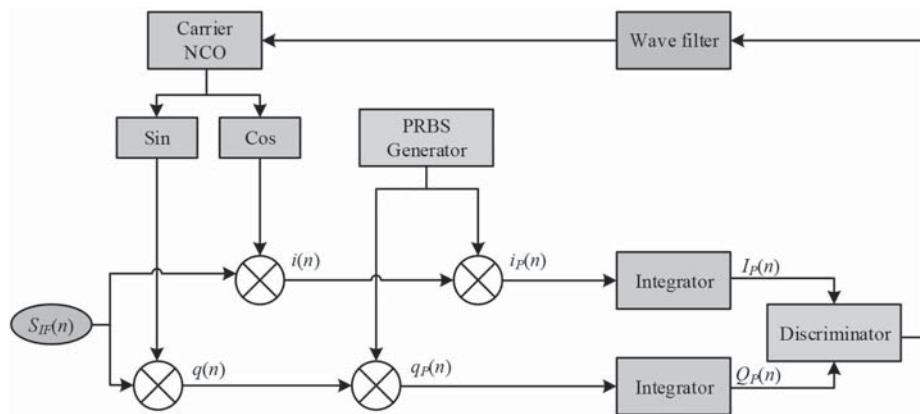


Figure 2 Carrier tracking loop of TC-OFDM.

3. DESIGN OF ADAPTIVE KALMAN CARRIER TRACKING ALGORITHM

3.1 TC-OFDM-OFDM Receiver Tracking Loop Design

The TC-OFDM positioning system independently developed by China achieves high-precision indoor positioning without interfering with other communication services. The positioning receiver is the core component of the TC-OFDM system, and the baseband signal processing module is the core component of the receiver. The signal processing system of the receiver is shown in Figure 1.

A key function of the receiver signal processing block is signal tracking. Signal tracking is divided into carrier tracking and pseudo-code tracking. The process involves using the carrier loop in the tracking loop to track the signal carrier after capturing the positioning signal, then calculating the coherent integration and stripping residual filtering in the tracking channel, and adjusting the tracking loop. The path

sum is synchronized by bit synchronization, and then the demodulation of pseudocode information and the calculation of pseudorange information are completed, thereby arriving at the positioning solution. The design of the carrier tracking loop has a decisive effect on the positioning effect, and its main components include a mixer, a phase detector/frequency discriminator, an integrator, and a carrier oscillator. Generally, the tracking loop can be divided into two types: phase-locked loop (PLL) and frequency-locked loop (FLL) according to the type of discriminator. Phase-locked loops generally use phase discriminators and partial PLLs. The frequency discriminator is used as an auxiliary in the loop, and the frequency discriminator is generally used in the FLL. The carrier tracking loop of the TC-OFDM receiver is shown in Figure 2.

In Figure 2, $S_{IF}(n)$ is the digital intermediate frequency signal, the $i(n)$ and $q(n)$ is the mixing result after carrier stripping, $I_P(n)$ and the sum $Q_P(n)$ is the operation result of coherent integration, used to calculate the discrimination result, and the discrimination result is input to the carrier

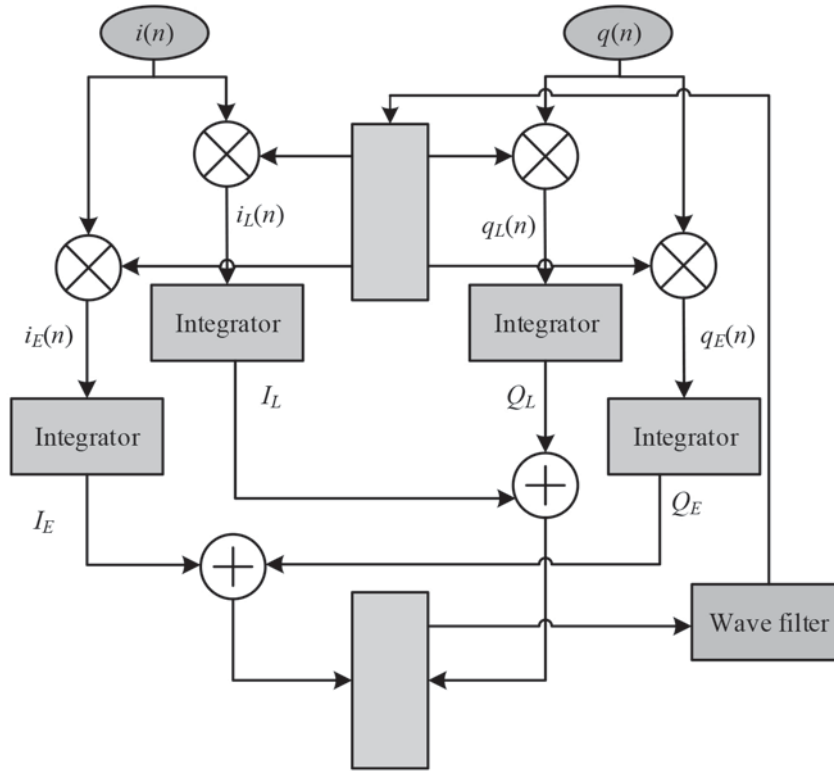


Figure 3 Code tracking loop of TC-OFDM.

oscillator through the loop filter to synchronize the local carrier and the signal carrier to complete the tracking of the signal carrier. The purpose of the coherent integration operation is to increase the signal-to-noise ratio, and the duration is generally one chip period, but in a strong interference or weak signal environment, the coherent integration duration needs to be increased. The coherent integral gain G is calculated with Formula (1).

$$G = 10 \lg N_c = 10 \lg(f_s \cdot t_c) \quad (1)$$

In Formula (1), N_c is the number of mixing results, f_s the sampling frequency, and t_c the coherent integration time. When tracking continuous-type signals, the loop duration is usually t_{ep} equal to the coherence duration. When tracking the discontinuous signal, the correlation integration of the loop is only calculated in the downlink time slot, and the coherent integration time at this time is shown in Formula (2).

$$t_c = \omega \cdot t_{ep} \quad (2)$$

In Formula (2), ω is Duty Ratio, which is the proportion of downlink time slots relative to signal subframes. The coherent integral gain of discontinuous signal tracking is shown in Formula (3).

$$G = 10 \lg(\alpha f_s \cdot t_{ep}) \quad (3)$$

Formula (3) shows that if the t_{ep} multiplication $1/\omega$ is multiplied, the obtained coherent integral gain is equal to the continuous signal. When t_{ep} increases, the carrier pulling range of the loop decreases, which may lead to the deviation of the adjustment direction of the carrier oscillator. Therefore, it is necessary to comprehensively consider the signal-to-noise ratio and the pulling range of the carrier loop that

will be selected. It is difficult for the tracking loop of the discontinuous signal to obtain a consistently high coherent integral gain, resulting in a low final positioning accuracy. The main function of the code tracking loop is to reproduce the pseudocode locally and perform a coherent integration operation on the pseudocode of the signal, and then adjust the code oscillator to track the pseudocode of the signal [16]. Its main components are: a pseudo code generator, an integrator, a code phase detector, a code oscillator, etc., which are usually designed with a Delay-Locked Loop (DLL). The code tracking loop of the TC-OFDM-OFDM receiver is shown in Figure 3.

The pseudo-code generator locally generates 3-way pseudo-codes leading (E), immediate (P) and lagging (L), wherein the phase of the P code is synchronized with the signal pseudo-code, the EP phase difference is equal to the PL phase difference. The difference is taken as the correlator spacing, which is 1/2 chip (chips) in the receiver. There are 6 correlators in each tracking channel of the receiver, the mixing result and the 3-channel pseudocode are simultaneously performed as a coherent integral operation. The operation result is obtained with Formula (4).

$$\begin{cases} E(n) = |\text{sinc}(f_e t_c)| a R_{\eta(E)} \\ P(n) = |\text{sinc}(f_e t_c)| a R_{\eta(P)} \\ L(n) = |\text{sinc}(f_e t_c)| a R_{\eta(L)} \end{cases} \quad (4)$$

In Formula (4), R represents the pseudo-code autocorrelation functions, $\eta(E)$, and $\eta(P)$, $\eta(L)$ represent the phase error between the locally replicated pseudo-code and the signal pseudo-code. Only when the phases of the immediate pseudocode and the signal pseudocode are synchronized, are the coherent integrals of the leading and lagging pseudocodes

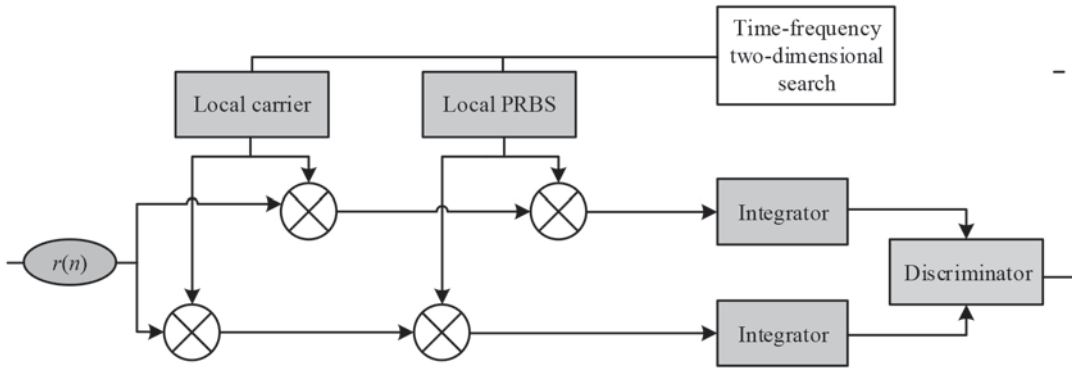


Figure 4 Open loop tracking loop with time-frequency two-dimensional search.

equal, so the phase difference between the instant pseudocode and the signal pseudocode can be indicated by the coherent integration of the lagging pseudocode of the leading pseudocode η' , as shown in Formula (5).

$$\eta' = \frac{E - L}{E + L}(1 - d) \quad (5)$$

Formula (5) is denoised by the filter, the code oscillator adjusts the rate of the local duplication pseudo code to synchronize with the signal pseudo code, thus completing the tracking of the signal pseudo code. The last step of the positioning receiver is ranging positioning. The parameters used in common ranging positioning technologies include time difference of arrival, time of arrival, and angle of arrival. Of these, the time difference of arrival has the highest positioning accuracy and is less difficult to implement. Therefore, TC-OFDM uses the time difference of arrival as the ranging and positioning parameters. The arrival time difference in the TC-OFDM system is the time difference between the various base station signals acquired by the receiver. The current k calculation formula is shown in Formula (6).

$$Td^{ij} = (\eta_i - \eta_j) \cdot f_\eta^{-1} \quad (6)$$

In Formula (6), Td^{ij} represents the arrival time difference of the two signals of the receiver, η_i is i the signal pseudo code phase η_j of the tracking channel, is the signal pseudo code phase of the tracking channel j , and f_η represents the baud rate of the signal pseudo code. After the stable tracking of the positioning signal is achieved, the position information of the signal source base station can be obtained by demodulating the message information of the positioning signal. When the number of stable tracking signals reaches 4 or more, they are calculated from the message information of each tracking signal (x_1, y_1, z_1) , (x_2, y_2, z_2) , and (x_3, y_3, z_3) then (x_4, y_4, z_4) equations can be constructed to calculate the position information of the receiver, as shown in Formula (7).

$$\begin{cases} c \cdot Td^{12} = \sqrt{(x - x_2)^2 + (y - y_2)^2 + (z - z_2)^2} \\ \quad - \sqrt{(x - x_1)^2 + (y - y_1)^2 + (z - z_1)^2} \\ c \cdot Td^{13} = \sqrt{(x - x_3)^2 + (y - y_3)^2 + (z - z_3)^2} \\ \quad - \sqrt{(x - x_1)^2 + (y - y_1)^2 + (z - z_1)^2} \\ c \cdot Td^{14} = \sqrt{(x - x_4)^2 + (y - y_4)^2 + (z - z_4)^2} \\ \quad - \sqrt{(x - x_1)^2 + (y - y_1)^2 + (z - z_1)^2} \end{cases} \quad (7)$$

In Formula (6), c is the speed of light.

3.2 Open-Loop Tracking Loop and Adaptive Kalman Filter Algorithm Design

When the 5G communication adopts the TDD system, the positioning signal is broadcast only in the downlink time slot, and the DutyRatio is small. The traditional closed-loop tracking method cannot achieve stable signal tracking, while the open-loop tracking method does not have similar problems. Open-loop tracking does not have its own feedback mechanism. After the receiver captures the positioning signal, the initial phase and carrier frequency of the signal are obtained. On this basis, the time-frequency two-dimensional search of signal parameters is performed to obtain the code phase index and frequency index of the positioning signal [17]. The design of the open-loop tracking system is shown in Figure 4.

After the code phase and frequency index are obtained, a discriminator is needed to accurately estimate the code phase error and carrier frequency. The code phase error and its variance V_η are calculated by using the lead-minus-lag power discriminator η'_k , as shown in Formula (8).

$$\begin{cases} \eta'_k = \frac{P_{x-1,y}(k) - P_{x+1,y}(k)}{P_{x-1,y}(k) + P_{x+1,y}(k)} \eta_b + \eta_{x,k} - \eta_k^0 \\ V_\eta = \left(1 + \frac{1}{i_c \cdot C/N(1 - \eta_b)}\right) \frac{\eta_b}{2i_c \cdot C/N} \end{cases} \quad (8)$$

In Formula (8), $P_{x-1,y}(k)$, $P_{x+1,y}(k)$, represent the integral energy of the time-frequency two-dimensional search unit, $\eta_{x,k}$ represents the code phase delay of the time-frequency two-dimensional unit, η_k^0 represents the central code phase of the time-frequency two-dimensional search, and $P_{x+1,y}(k)$ represents the time-frequency two-dimensional adjacent units. The code phase interval, C/N indicates the carrier-to-noise ratio. The carrier frequency error and its variance V_f can be calculated by using the frequency discriminator f'_k , as shown in Formula (9).

$$\begin{cases} f'_k = \frac{(\pi f_b t_c)^3 \cdot (P_{x,y+1} - P_{x,y-1})}{[1 - \pi f_b t_c \cos(2\pi f_b t_c) - \cos(2\pi f_b t_c)] \cdot 2\pi f_b t_c P_{x,y}} + f_{y,k} - f_k^0 \\ V_f = \left(1 + \frac{\mu_0}{i_c \cdot C/N}\right) \frac{\mu_1}{4i_c \cdot C/N} \\ \mu_0 = \frac{1 - \sin^2(2\pi f_b t_c)}{2[1 - \cos(2\pi f_b t_c)] \sin^2(2\pi f_b t_c)} \\ \mu_1 = \frac{f_b^2 [1 - \cos(2\pi f_b t_c)]}{[\sin(2\pi f_b t_c) - \cos(2\pi f_b t_c)]^3} \end{cases} \quad (9)$$

In Formula (9), $P_{x,y+1}$, $P_{x,y-1}$, $P_{x,y}$ represent the integral energy of the time-frequency two-dimensional search unit,

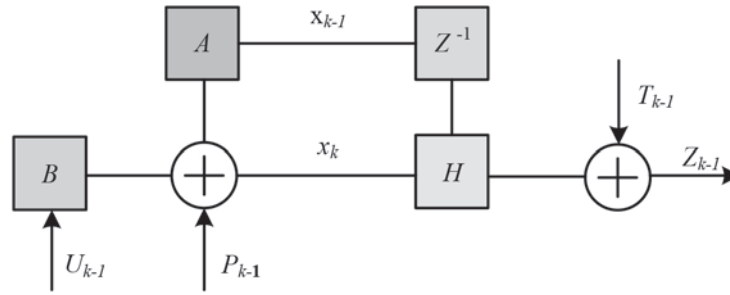


Figure 5 Discrete Kalman filter model.

$f_{y,k}$ represents the frequency offset of the time-frequency two-dimensional unit, f_k^0 represents the center carrier frequency of the time-frequency two-dimensional search, and f_b represents the time-frequency two-dimensional adjacent units frequency interval. The carrier phase error and its variance V_θ can be calculated using the four-quadrant Arctan function θ'_k , as shown in Formula (10).

$$\begin{cases} \theta'_k = \arctan(I_{x,y}(k), Q_{x,y}(k)) \\ V_\theta = \left(1 + \frac{1}{2t_c C/N}\right) \cdot \frac{1}{4\pi^2 t_c C/N} \end{cases} \quad (10)$$

It can be seen that the signal-to-noise ratio is related to the calculation results of η'_k , f'_k and θ'_k , thus affecting the final positioning accuracy. In order to reduce the influence of noise on the identification results, KF is used for filtering. KF is widely used for the optimal estimation of linear discrete systems, and relies on estimators with prediction and correction functions. On the one hand, the input signal is predicted based on the system model, and on the other hand, the observed value of the input signal is corrected based on the measurement model. If the system model parameters are determined and the process noise and measurement noise are known, the KF can achieve the optimal estimation, otherwise it cannot do so. However, the positioning signal of the TC-OFDM system is broadcast intermittently, and the traditional KF algorithm cannot achieve efficient and precise positioning. The adaptive adjustment of the filter gain is achieved, thereby effectively improving the positioning accuracy. In traditional KF, a linear discrete system is established as shown in Figure 5.

The state equation of KF can be obtained by using the matrix vector as shown in Formula (11).

$$x_k = BU_{k-1} + Ax_{k-1} + P_{k-1} \quad (11)$$

In Formula (11), B represents $k-1$ the relationship matrix between the system input and the system state at A time, the state transition matrix from time to time, and P_{k-1} the $k-1$ process k noise. The measurement equation of KF is shown in Formula (12).

$$Z_k = T_k + Hx_k \quad (12)$$

In Formula (12), T_k is the measurement noise vector, H and is the relationship transition matrix between the system state vector and the observed quantity at time k . The KF algorithm can be divided into two stages: prediction stage and correction stage. In the prediction stage, k , the state value at time, can be estimated according to the state equation of the system and $k-1$ the state value at time, as shown in Formula (13).

$$\begin{cases} \tilde{x}_k^- = BU_{k-1} + A\tilde{x}_{k-1} \\ F_k^- = BF_{k-1} + Q_{k-1} \end{cases} \quad (13)$$

In the Formula (13), F_{k-1} represents the posterior estimation error covariance matrix, and F_k^- represents the moment at $k-1$, the prior estimation error covariance matrix represents the moment, and the reliability used to evaluate \tilde{x}_k^- represent k the Q_{k-1} process noise covariance matrix. The correction stage corrects the prior estimates obtained in the prediction stage, as shown in Formula (14).

$$\begin{cases} G_k = (R_k + HF_k^-H^T)^{-1}F_k^-H^T \\ \tilde{x}_k = G_k(Z_k - H\tilde{x}_k^-) + \tilde{x}_k^- \\ F_k = F_k^-(I - G_kH) \end{cases} \quad (14)$$

In the Formula (14), G_k represents the KF total gain, \tilde{x}_k represents k the best estimated state value of the F_k state vector at the moment, x represents k the a posteriori estimation error covariance matrix at the moment, and R_k represents k the measurement noise covariance matrix at the moment. When estimating the measurement noise variance, combined with the open-loop tracking loop discriminator design, the CNR needs to be measured first. When tracking a certain signal stably, CNR can be calculated using the correlation function of the coherent integration results of the two tracking channels, as shown in Formula (15).

$$\begin{cases} I_P(n) = \tau_I + \beta_\tau \cos \phi_e \sqrt{2(C/N)t_c} \\ Q_P(n) = \tau_Q + \beta_\tau \sin \phi_e \sqrt{2(C/N)t_c} \end{cases} \quad (15)$$

In the Formula (15), $I_P(n)$ and $Q_P(n)$ is the coherent integration result, τ_I and τ_Q are the zero-mean Gaussian noise of variance. When tracking a continuous, intermittent positioning signal, CNR can be estimated by counting the results of two coherent integrations. The defined Z value is as shown in Formula (16).

$$Z = \frac{\sum_{n=1}^M (I_d^2(n) + Q_d^2(n))}{\sum_{n=1}^M (I_u^2(n) + Q_u^2(n))} \quad (16)$$

In the Formula (16), $I_d(n)$, $Q_d(n)$ represents the coherent integration result of downlink time slot tracking channel, and $I_u(n)$, $Q_u(n)$ represents the coherent integration result of uplink time slot tracking channel, then the calculation of CNR is shown in Formula (17).

$$C/N = \left(Z \cdot \frac{M}{M+2} - 1\right) \cdot t_c^{-1} \quad (17)$$

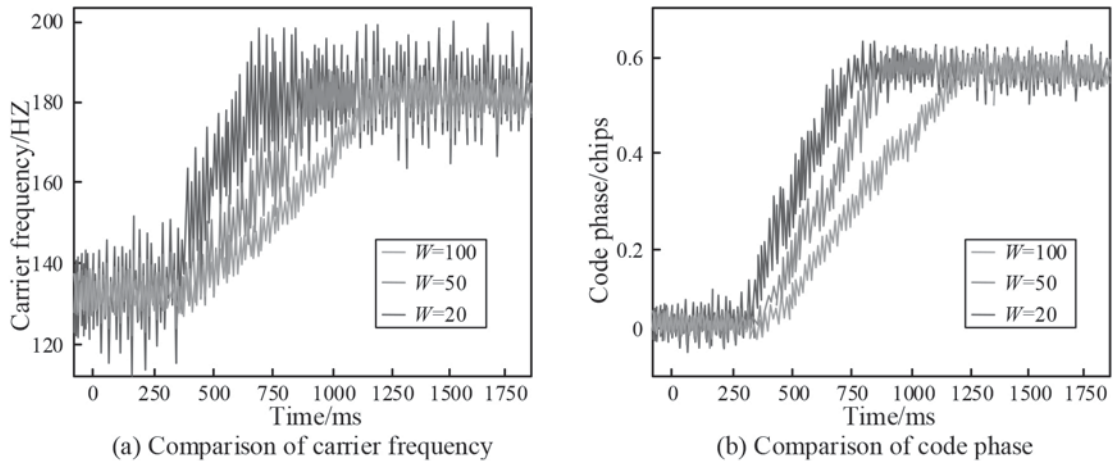


Figure 6 Carrier frequency and code phase tracking results at different window lengths.

After the CNR is obtained, it can be combined with the real-time estimate calculated by the discriminator's estimation method R_k . When estimating the process noise variance, firstly, the residual is calculated according to the measured actual value and the predicted value, as shown in Formula (18).

$$r_k = Z_k - \tilde{Z}_k^- = T_k + Hx_k - H\tilde{x}_k^- = T_k + H_kx_k^- \quad (18)$$

In the Formula (18), r_k represents the measurement residual, Z_k represents the actual measured value, \tilde{Z}_k^- represents the predicted measured value, and $\tilde{x}_k^- = H\tilde{x}_k^-$ represents the one-step measurement error, and $\tilde{x}_k^- = x_k - \tilde{x}_k^-$. The variance of the measurement residual is V_{r_k} dynamically estimated by using the windowing estimation method, as shown in Formula (19).

$$V'_{r_k} = \begin{cases} \frac{1}{W} \sum_{i=k-W+1}^k r_i r_i^T & k > W \\ \frac{1}{k} r_k r_k^T + \frac{k-1}{k} V'_{r_{k-1}} & k \leq W \end{cases} \quad (19)$$

In the Formula (19), it V_{θ} represents k the variance of measurement residuals at time, $V'_{r_{k-1}}$ represents the variance $k-1$ of measurement residuals at time, and W represents the length of the sliding window. Whether the length is suitable or not has an important influence on the final tracking performance. Then the estimation of the variance of V_{r_k} the residual is shown in r_k Formula (20).

$$\begin{aligned} V_{r_k} &= E(r_k r_k^T) = E(T_k T_k^T) + E(x_k^- x_k^{-T}) H H^T \\ &= R_k + H F_k^- H^T \end{aligned} \quad (20)$$

By substituting Equation (20) into Equation (14), the process noise covariance matrix can be obtained as shown in Equation (21).

$$Q_{k-1} = G_k V_{r_k} G_k^T + F_k - A F_{k-1} \quad (21)$$

When the KF state is relatively stable, there are $G_k \approx G_{k-1}$, $F_k \approx F_{k-1} \approx 0$, so the process noise covariance matrix can be simplified and calculated according to Formula (21), as shown in Formula (22).

$$\tilde{Q}_{k-1} = G_{k-1} V_{r_k} G_{k-1}^T \quad (22)$$

This enables real-time estimation of process noise variance.

4. PERFORMANCE ANALYSIS OF ADAPTIVE KALMAN CARRIER TRACKING ALGORITHM

4.1 Adaptive Kalman Filtering Algorithm Simulation Verification

The effective tracking of the positioning signal can be achieved by filtering the parameters initially estimated by the open-loop tracking loop with the improved adaptive KF. When estimating the carrier parameters of the positioning signal, the carrier phase error, angular frequency error and its change rate of the positioning signal, and the local signal are used as the state vector of KF; when estimating the pseudocode parameters of the positioning signal, the difference between the positioning signal and the local signal is used. The code phase difference and code rate difference are used as the state vector of KF. In order to verify the performance of the open-loop tracking loop (AKF-OL) based on adaptive Kalman filtering proposed in the research, the real TC-OFDM-OFDM signal is obtained by using a signal collector, and the simulation verification and performance comparison analysis of the tracking loop is carried out. First, adjust the length of the sliding window W used to estimate the variance of the measurement residual V_{r_k} , verify W the signal tracking effect of different loops, and determine the parameter settings under the best effect. The signal-to-noise ratio of the simulation environment is -24 dB, and the values are 20, 50, and 100 respectively. When the loop tracking state is stable, noise is artificially added. The tracking loop observation results are shown in Figure 6.

It can be seen from Figure 6 that the jitter trends of the code phase and carrier frequency tend to be gradual with the increase of W . At the same time, the changes in the accuracy and dynamic response speed of AKF-OL are considered. In order to further determine W the optimal value and the value of gradient adjustment W , the corresponding changes of the carrier frequency standard deviation and the code phase standard deviation are examined. The results are shown in Figure 7.

It can be seen from the change curve in Figure 7 that the carrier frequency standard deviation and the code phase

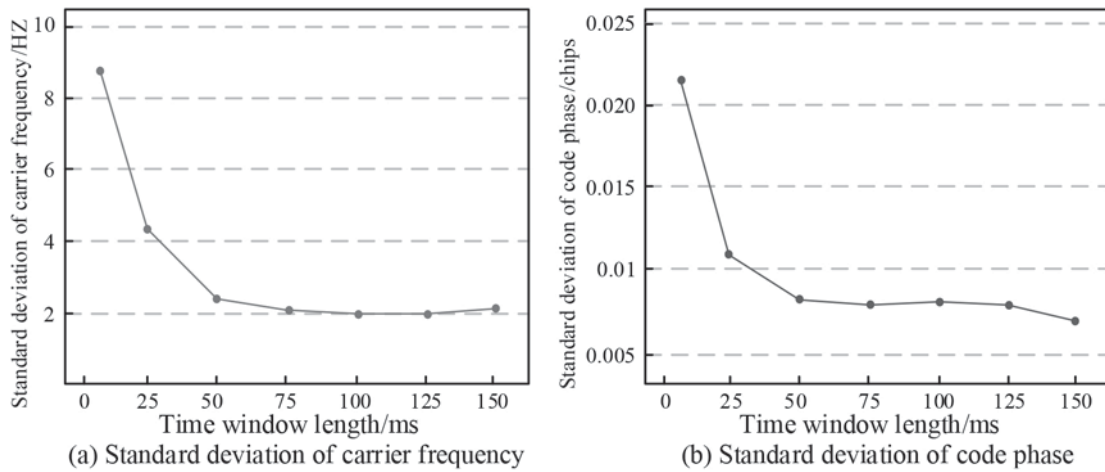


Figure 7 Carrier frequency and code phase standard deviation at different W .

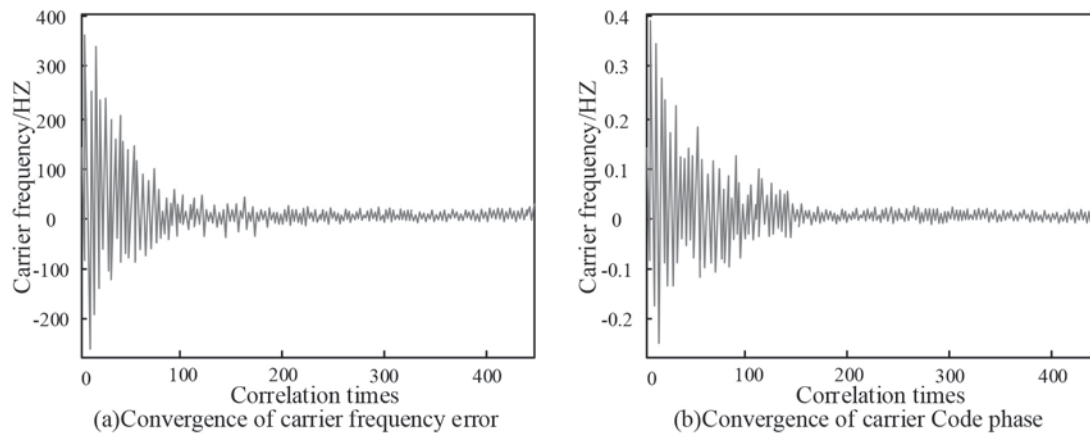


Figure 8 Convergence of carrier frequency error and code phase when $W = 50$.

standard deviation W have an obvious downward trend when the value of σ is less than 50, and when W the value of σ is greater than 50, the downward trend of the two tends to be more gradual, and there is even an upward trend. Therefore, according to the adjustment gradient, combined with the tracking accuracy and response speed of the loop, the W value can be determined as 50. When it W is 50, the carrier frequency error converges, as shown in Figure 8.

It can be seen from Figure 8 that when the number of correlations is close to 100, the carrier frequency error approaches 0, and when the number of correlations approaches 150, the code phase error approaches 0, the convergence effect is good, and the loop enters stable tracking. After the state, the carrier frequency and code phase errors are relatively stable, and the jitter is small. Therefore, the AKF-OL design can achieve effective tracking of TC-OFDM signals.

4.2 Performance Comparison of Adaptive Kalman Filtering Algorithms

In order to verify the tracking performance of the proposed AKF-OL for positioning signals, the AKF-OL, the open-loop tracking structure based on the basic KF (KF-OL), and the closed-loop tracking structure based on the improved adaptive

KF (AKF-CL) were tested. TC-OFDM signal tracking simulation was carried out to compare the tracking effect of each tracking method under different uplink-downlink timeslot ratios and the tracking effect under different SNR. Figure 9 shows the variation of carrier frequency error and code phase error of different tracking structures at a certain uplink-downlink time slot ratio.

As can be seen from Figure 9, when the SNR is -24 dB, although the traditional closed-loop tracking structure adopts the adaptive KF algorithm, it is limited by the greater influence of the DutyRatio, and the tracking accuracy of the TC-OFDM signal is low. Also, with the increase of the uplink-downlink time slot ratio, the accuracy has an obvious downward trend. The open-loop tracking structure using the traditional KF algorithm can estimate the real-time signal parameters from the known tracking mode state value. The open-loop tracking structure based on the self-adaptive KF algorithm designed in this research can accurately reflect the noise characteristics by updating the process noise and measurement noise in real time. Figure 10 shows the carrier frequency and code phase estimation errors of the tracking methods for the TC-OFDM when the SNR is -30 dB.

As can be seen from Figure 10, the carrier frequency error of AKF-OL is the smallest, the overall value is between $[-5, 5]$, and the code phase error is also the smallest. The

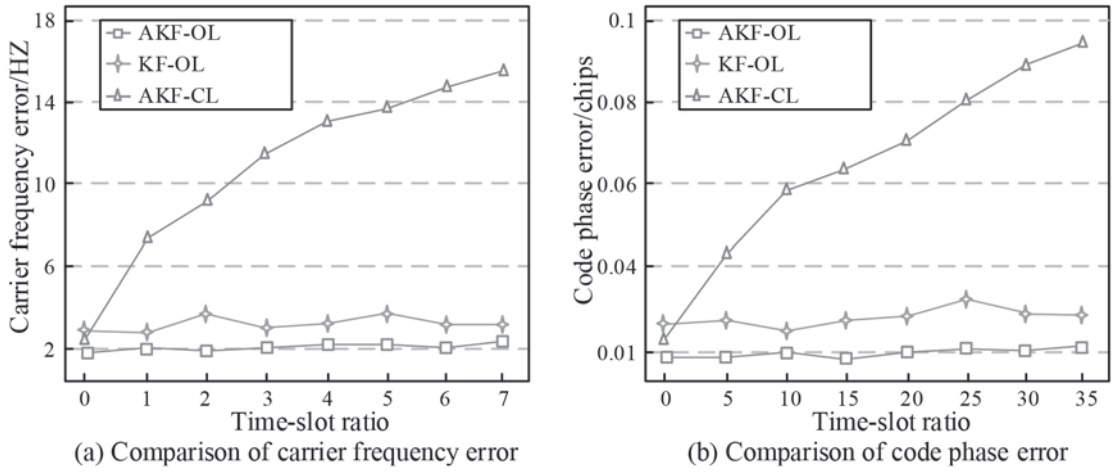


Figure 9 Carrier frequency error and code phase error at different slot ratios.

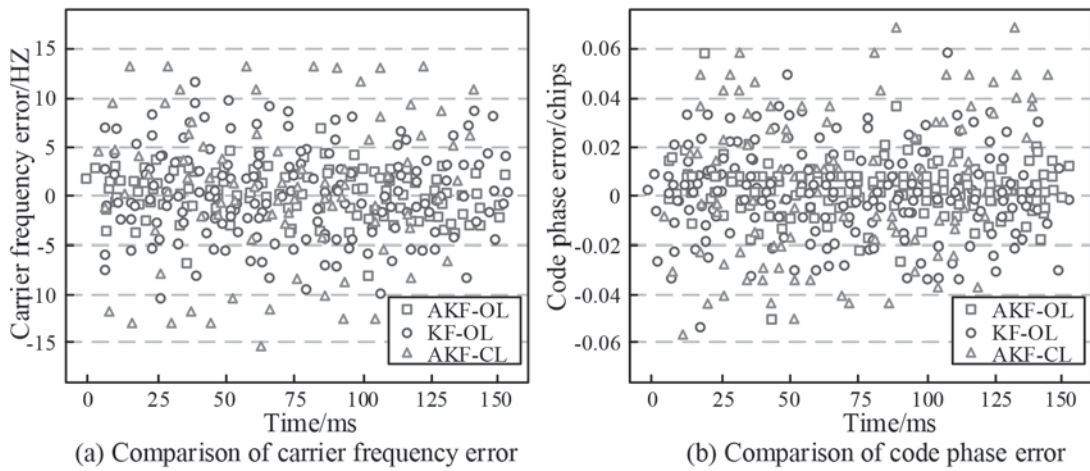


Figure 10 Carrier frequency and code phase error of different loops.

overall value is between $[-0.020, 0.02]$; the frequency and code phase errors of KF-OL are slightly greater than those of AKF-OL, where the overall carrier frequency error is between $[-10, 10]$, and the overall code phase error is between $[-0.04, 0.04]$; the carrier frequency of AKF-OL and the code phase error is the largest. Therefore, the proposed AKF-OL tracking structure has the highest accuracy and the best performance when tracking the TC-OFDM signal; the KF-OL tracking structure based on the traditional KF algorithm is less accurate than the AKF-OL, and will be more accurate when the CNR changes. The AKF-CL tracking structure also adopts adaptive KF because the closed-loop structure has poor adaptability when tracking intermittent signals, so the tracking accuracy is the lowest. To sum up, the AKF-OL tracking structure has high precision and fast convergence speed when tracking the TC-OFDM signal, and can achieve stable tracking of the positioning signal.

5. CONCLUSION

Signal shading during indoor positioning leads to low accuracy. However, 5G technology has gradually matured, and signals using the TDD format are becoming more and more common, requiring the TC-OFDM system to make

corresponding improvements to the features of TDD signals. Under the TDD system, the TC-OFDM positioning signal is broadcast only in the downlink, which is intermittent, so the traditional closed-loop tracking structure cannot achieve effective tracking. Therefore, the open-loop structure is used to design the tracking loop of the TC-OFDM receiver. After the preliminary estimation of the carrier frequency and code phase, the improved KF algorithm is used for the filtering process to estimate the measurement noise of the tracking loop in real time and the statistical characteristics of process noise, so as to achieve stable tracking of TC-OFDM signals. In the simulation experiment, the optimal window length was determined according to the variation of carrier frequency and code phase error, and then the good convergence performance of this tracking loop design was verified. Results show that, compared with other tracking structures such as AKF-CL and KF-OL, the AKF-OL, the SNR = -24dB designed in the study is less affected by the time slot ratio, the signal tracking effect is stable, and the accuracy is the highest. With SNR = -30dB, the carrier frequency and code phase error range of AKF-OL is the smallest, so the accuracy is the highest, and less affected by CNR. This research is related to the stable, indoor positioning, so further research is required to study the performance of the tx signal tracking when there is dynamic scene switching.

REFERENCES

1. Li W., Zhang Q., Luo Y., et al. 2020. Development of a new multifunctional induced polarization instrument based on remote wireless communication technology. *IEEE Access*, 8: 100415–100425.
2. Xue X., Lin X., Yang C., et al. 2020. An improved indoor positioning technique based on receiving signal's strength. *Mobile Information Systems*, 2020(4): 1–10.
3. Liu W., Bian X., Deng Z., et al. 2018. A novel carrier loop algorithm based on maximum Likelihood Estimation (MLE) and Kalman Filter (KF) for weak TC-OFDM-OFDM signals. *Sensors*, 18(7): 1–22.
4. Han C., Bai Y., Si J. 2018. Joint carrier synchronization algorithm by open-loop acquisition and closed-loop tracking in high-dynamic environments. *Xibei Gongye Daxue Xuebao/Journal of Northwestern Polytechnical University*, 36(6): 1232–1235.
5. Dong S., Momson I., Kshattray S, et al. 2020. A 10-Gb/s 180-GHz phase-locked-loop minimum shift keying receiver. *IEEE Journal of Solid-State Circuits*, 56(3): 681–693.
6. Mo J., Deng Z., Jia B., et al. 2018. A novel FLL-assisted PLL with fuzzy control for TC-OFDM-OFDM carrier signal tracking. *IEEE Access*, 6: 52447–52459.
7. Yang R., Huang J., Zhan X., et al. 2021. Decentralized FLL-assisted PLL design for robust GNSS carrier tracking. *IEEE Communications Letters*, 25(10): 3379–3383.
8. Xu T., Gao F., Wang X., et al. 2019. A carrier synchronization method for global synchronous pulsewidth modulation application using phase-locked loop. *IEEE Transactions on Power Electronics*, 34(11): 10720–10732.
9. Liu M., Chen Q., Wu Y., et al. 2018. Joint carrier synchronization and symbol timing for MQAM in non-cooperation communication systems. *Xi'an Dianzi Keji Daxue Xuebao/Journal of Xidian University*, 45(1): 17–22.
10. Cheng Y., Chang Q. 2019. A Coarse-to-fine adaptive kalman filter for weak GNSS signals carrier tracking. *IEEE Communications Letters*, 23(12): 2348–2352.
11. Cheng Y., Chang Q. 2020. A carrier tracking loop using adaptive strong tracking kalman filter in GNSS receivers. *IEEE Communications Letters*, 24(12): 2903–2907.
12. Chen C., Chang G., Luo F., et al. 2019. Dual-frequency carrier smoothed code filtering with dynamical ionospheric delay modeling. *Advances in Space Research*, 63(2): 857–870.
13. Tang X., Chen X., Pei Z., et al. 2019. The explicit tuning investigation and validation of a full kalman filter-based tracking loop in GNSS receivers. *IEEE Access*, 7: 111487–111498.
14. Cheng Y., Chang Q., Wang H., et al. 2019. A two-stage Kalman filter-based carrier tracking loop for weak GNSS Signals. *Sensors*, 19(6): 1–16.
15. Jin T., Yuan H., Ling K.V., et al. 2020. Differential Kalman filter design for GNSS open loop tracking. *Remote Sensing*, 12(5): 1–24.
16. Tran V.T., Shivaramaiah N.C., Nguyen T.D., et al. 2018. GNSS receiver implementations to mitigate the effects of commensurate sampling frequencies on DLL code tracking. *GPS Solutions*, 22(1): 1–24.
17. Du W., Qiang F., Wang H. 2017. Subsynchronous oscillations caused by open-loop modal coupling between VSC-Based HVDC line and power system. *IEEE Transactions on Power Systems*, 33(4): 3664–3677.